Differential regulation of HMG-CoA reductase and Insig-1 by enzymes of the ubiquitin-proteasome system

Yien Che Tsai[a], Gil S. Leichner[b], Margaret M. P. Pearce[c,*], Gaye Lynn Wilson[a], Richard J. H. Wojcikiewicz[c], Joseph Roitelman[b], and Allan M. Weissman[a]

[a]Laboratory of Protein Dynamics and Signaling, National Cancer Institute, Frederick, MD 20712; [b]Bert W. Strassburger Lipid Center, Sheba Medical Center, Tel Hashomer 52621, and Department of Human Genetics and Biochemistry, Sackler Faculty of Medicine, Tel Aviv University, Tel Aviv 69978, Israel; [c]Department of Pharmacology, SUNY Upstate Medical University, Syracuse, NY 13210

ABSTRACT **The endoplasmic reticulum (ER)–resident enzyme 3-hydroxy-3-methylglutaryl CoA (HMG-CoA) reductase catalyzes the rate-limiting step in sterol production and is the therapeutic target of statins. Understanding HMG-CoA reductase regulation has tremendous implications for atherosclerosis. HMG-CoA reductase levels are regulated in response to sterols both transcriptionally, through a complex regulatory loop involving the ER Insig proteins, and posttranslationally, by Insig-dependent protein degradation by the ubiquitin-proteasome system. The ubiquitin ligase (E3) gp78 has been implicated in the sterol-regulated degradation of HMG-CoA reductase and Insig-1 through ER-associated degradation (ERAD). More recently, a second ERAD E3, TRC8, has also been reported to play a role in the sterol-accelerated degradation of HMG-CoA reductase. We interrogated this network in *gp78*$^{-/-}$ mouse embryonic fibroblasts and also assessed two fibroblast cell lines using RNA interference. Although we consistently observe involvement of gp78 in Insig-1 degradation, we find no substantive evidence to support roles for either gp78 or TRC8 in the robust sterol-accelerated degradation of HMG-CoA reductase. We discuss factors that might lead to such discrepant findings. Our results suggest a need for additional studies before definitive mechanistic conclusions are drawn that might set the stage for development of drugs to manipulate gp78 function in metabolic disorders.**

Monitoring Editor
Thomas Sommer
Max Delbruck Center
for Molecular Medicine

Received: Aug 29, 2012
Revised: Oct 4, 2012
Accepted: Oct 9, 2012

INTRODUCTION

Atherosclerosis is a leading cause of mortality in the developed world (Lloyd-Jones *et al.*, 2009). The enzyme 3-hydroxy-3-methylglutaryl CoA reductase (HMGCR) catalyzes the rate-limiting formation of mevalonate (MVA), the first committed precursor for the metabolic pathway in which cholesterol and many essential nonsterol isoprenoids are produced (Goldstein and Brown, 1990). HMGCR is a polytopic glycoprotein resident in the endoplasmic reticulum (ER). It includes an N-terminal region of eight transmembrane spans that contains a sterol-sensing domain (Liscum *et al.*, 1983a; Roitelman *et al.*, 1992). Targeting of HMGCR represents a major therapeutic approach to lowering plasma cholesterol levels and preventing atherosclerosis (reviewed in Steinberg, 2006), as evidenced by the therapeutic effects of statins, which are competitive inhibitors of HMGCR. Given the extraordinary public health implications, it is critical to understand how HMGCR is regulated.

The levels of HMGCR in mammalian cells are negatively regulated by cholesterol both transcriptionally and posttranslationally. At low cholesterol levels, HMGCR transcription is stimulated by binding of sterol regulatory element–binding proteins (SREBPs) to its promoter. To reach the nucleus, SREBPs, which are synthesized as

This article was published online ahead of print in MBoC in Press (http://www.molbiolcell.org/cgi/doi/10.1091/mbc.E12-08-0631) on October 19, 2012.

*Present address: Department of Biology, Stanford University, Stanford, CA 94305.

Address correspondence to: Joseph Roitelman (Joseph.Roitelman@sheba.health.gov.il), Allan M. Weissman (weissmaa@mail.nih.gov).

Abbreviations used: 25-HC, 25-hydroxycholesterol; ER, endoplasmic reticulum; ERAD, ER-associated degradation; HMGCR, 3-hydroxy-3-methylglutaryl CoA reductase; LPDS, lipoprotein-deficient serum; MEF, mouse embryonic fibroblast; MVA, mevalonate; SCAP, SREBP cleavage-activating protein; SREBP, sterol regulatory element–binding protein.

ER-membrane–embedded precursors, are transported to the Golgi, where they are cleaved, releasing a soluble transcription activator. The proteolytic activation of SREBPs depends on SREBP cleavage-activating protein (SCAP), another polytopic membrane protein with a sterol-sensing domain that associates with and escorts the SREBP precursors from the ER to the Golgi. When the level of cellular cholesterol increases, SCAP binds either one of two closely related ER-resident proteins, Insig-1 and Insig-2. This retains SCAP, together with the inactive SREBP precursors, in the ER, preventing the generation of transcriptionally active SREBPs (reviewed in Goldstein *et al.*, 2006)

At a posttranslational level, cholesterol and MVA-derived metabolites regulate the degradation of HMGCR (Faust *et al.*, 1982; Edwards *et al.*, 1983; Nakanishi *et al.*, 1988). Thus, when cholesterol/MVA levels are low, HMGCR is a rather stable protein. However, when cholesterol/MVA levels increase, HMGCR is rapidly degraded by the ubiquitin-proteasome system (Ravid *et al.*, 2000) through ER-associated degradation (ERAD; Hirsch *et al.*, 2004; Vembar and Brodsky, 2008). The metabolically regulated degradation of HMGCR has also been shown to involve Insig-1 and/or Insig-2 (Sever *et al.*, 2003a,b). It was proposed that these proteins act as scaffolds to recruit ER ubiquitin ligase(s) (E3s) to HMGCR in a sterol-dependent manner, stimulating ubiquitination and proteasomal degradation of HMGCR (Jo and Debose-Boyd, 2010).

In *Saccharomyces cerevisiae*, ubiquitination of an HMGCR orthologue, Hmg2p, is mediated by the polytopic RING finger ubiquitin ligase Hrd1p/Der3p (Hampton *et al.*, 1996), one of only two *S. cerevisiae* ERAD E3s (reviewed in Kostova *et al.*, 2007). In mammals there are >5, and possibly >20, ER-resident RING finger E3s (Neutzner *et al.*, 2011). The two most studied are the polytopic Hrd1p orthologues HsHrd1/Synoviolin, an E3 implicated in arthritis and the ubiquitin ligase for p53, and gp78, also known as the human tumor autocrine motility factor receptor or RNF45 (reviewed in Tsai and Weissman, 2010). gp78 is implicated in targeting the metastasis suppressor CD82/KAI11, as well as other proteins, for degradation (Tsai *et al.*, 2007). HsHrd1 was assessed for a role in the sterol-regulated degradation of HMGCR, with negative results (Nadav *et al.*, 2003; Kikkert *et al.*, 2004). On the other hand, Song *et al.* (2005) presented evidence in the transformed human fibroblast cell-line SV-589 that endogenous gp78, which they found to be associated with Insig-1, is responsible for the degradation of HMGCR in response to sterols. Using the same cell line, they subsequently reported that TRC8, another Insig-1–interacting ERAD E3 (Lee *et al.*, 2010), also plays a role in HMGCR degradation (Jo *et al.*, 2011). Moreover, TRC8 levels were reported to increase upon knockdown of gp78, presumably due to targeting of TRC8 for degradation by gp78 (Jo *et al.*, 2011).

Studies by Ye and colleagues showed that Insig-2 is a stable protein, whereas Insig-1 is a short-lived protein (Lee and Ye, 2004) that is targeted to ERAD by gp78 (Lee *et al.*, 2006). While our manuscript was being prepared, a study by Liu *et al.* (2012) in hepatocytes from liver-specific gp78-knockout mice, provided evidence for a role for gp78 in regulating the stability of both Insig-1 and Insig-2. This work in hepatocytes also reiterated the role of gp78 in the stimulated loss of HMGCR in response to sterols.

Independent of the foregoing studies, we assessed the role of gp78 in HMGCR degradation. Using primary mouse embryonic fibroblasts (MEFs) derived from *gp78*$^{-/-}$ embryos, we found no evidence directly implicating gp78 in HMGCR degradation. Similarly, we found no evidence for an effect of loss of gp78 expression on the sterol-stimulated decrease in HMGCR levels. To reconcile the apparent discrepancy with published reports (Song *et al.*, 2005; Jo *et al.*, 2011), we also assessed two cell lines, including SV-589 cells, and obtained results similar to those obtained in *gp78*$^{-/-}$ MEFs. Moreover, we did not find evidence for an effect of TRC8 on HMGCR degradation or for a significant increase in TRC8 protein in response to gp78 knockdown. We did, however, confirm the role of gp78 as an E3 for Insig-1 in MEFs, as well as in the cell lines. Thus further interrogation of the pathway leading to HMGCR degradation is required before firm mechanistic conclusions can be drawn.

RESULTS

Knockout of gp78 does not affect endogenous HMGCR degradation in mouse embryonic fibroblasts

We generated mice expressing a knockout allele for the gene encoding gp78 (*RNF45*) and derived MEFs that do not express gp78 (Figure 1, A–D). We previously reported that gp78 can target the tetraspanin metastasis suppressor CD82/KAI1 for degradation (Tsai *et al.*, 2007). Using these MEFs, we verified that gp78 is required for the degradation of endogenous CD82/KAI1 (Figure 1E). This also served as an internal control that gp78 function is lost in these cells.

We next examined the fate of endogenous HMGCR in two sets of paired *gp78*$^{-/-}$ (KO) and wild-type (WT) primary MEFs; each set was derived from a separate pregnancy. Given the varied and complex feedback mechanisms involved in regulating HMGCR expression, it was critical to examine HMGCR turnover directly. Although cycloheximide chase experiments can be used to assess protein stability, cycloheximide prevents sterol-accelerated HMGCR degradation and thus is of no utility for assessing HMGCR turnover (Chun *et al.*, 1990; Roitelman and Simoni, 1992; Roitelman *et al.*, 2004). We therefore used ^{35}S pulse-chase metabolic labeling and immunoprecipitation to quantitatively assess degradation of endogenous HMGCR in these MEFs. To increase HMGCR levels, cells were incubated in lipoprotein-deficient medium that also included compactin, a statin that inhibits HMGCR activity and thereby upregulates levels of HMGCR (Brown *et al.*, 1978), and supplemented with a low concentration of MVA to maintain cell viability (Kaneko *et al.*, 1978; Brown and Goldstein, 1980; medium B; see *Materials and Methods*). The cells were then pulse labeled for 30 min with [^{35}S] methionine and cysteine in the same medium. This was followed by a chase in "cold" medium B in the absence or presence of a mixture of sterols (2 µg/ml 25-hydroxycholesterol [25-HC] plus 20 µg/ml cholesterol; Roitelman and Simoni, 1992; Ravid *et al.*, 2000). At the indicated time points, endogenous HMGCR was immunoprecipitated with antiserum directed against its transmembrane region (Roitelman *et al.*, 1992). In the presence of added sterols, HMGCR was rapidly degraded in *gp78*$^{-/-}$ MEFs at the same rate as in WT MEFs (Figure 2, A and B). These are the first findings that directly address the role of gp78 in HMGCR degradation in cells completely lacking gp78 and demonstrate that sterol-accelerated degradation of HMGCR can occur independently of gp78 expression.

In previous studies carried out in SV-589 cells, which reported changes in the total levels of endogenous HMGCR in response to sterols upon manipulation of gp78 levels, HMGCR was largely assessed by immunoblotting without blocking new protein synthesis (Song *et al.*, 2005; Jo *et al.*, 2011). We conducted similar experiments in *gp78*$^{-/-}$ MEFs. HMGCR expression was up-regulated by sterol depletion and its levels were assessed by immunoblotting of postnuclear supernatants from detergent-lysed cells (lysates) using the same HMGCR monoclonal antibody (A9) previously used (Song *et al.*, 2005). Absence of gp78 (Figure 2C) had no significant effect on the decrease in HMGCR levels after the addition of sterols.

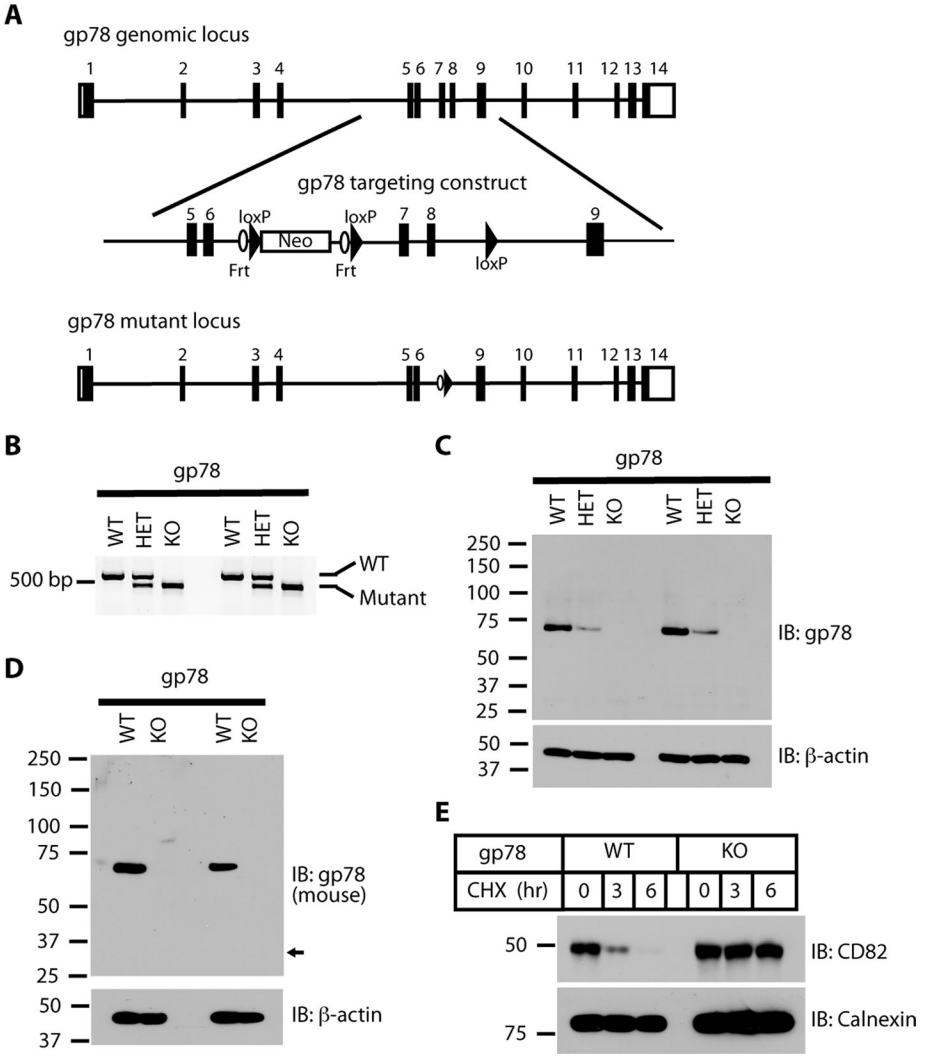

FIGURE 1: Characterization of gp78-knockout MEFs. (A) Schematic of gp78 gene-targeting strategy. The wild-type allele of murine *gp78* contains 14 exons. Excision of the sequences between the loxP sites deletes exons 7 and 8, which encode part of the most C-terminal transmembrane region and the adjacent RING finger domain of gp78. (B) Representative PCR analysis of genomic DNA from tails of wild-type (WT), heterozygous (HET), and *gp78*$^{-/-}$ (knockout [KO]) embryos. (C) Levels of gp78 protein in primary MEFs derived from gp78 WT, HET, or KO embryos were assessed by immunoblotting using gp78 Ab2. β-Actin was used as a control for equal loading. (D) To rule out the possibility that gp78$^{-/-}$ MEFs express a truncated form of gp78 terminating before exon 7 (see *Material and Methods*), levels of gp78 in primary MEFs from KO or WT embryos from the same litter were probed with affinity-purified rabbit antiserum directed against an N-terminal transmembrane region of mouse gp78 (aa 33–54; gp78 Ab3), which is encoded by exon 1. Arrow indicates the expected migration of truncated gp78 fragment if present. Results from two different sets of primary MEFs are shown. (E) Paired gp78 KO and WT MEFs were treated with 50 μg/ml cycloheximide (CHX) to inhibit protein synthesis, and degradation of CD82/KAI1 was monitored by immunoblotting with an antiserum recognizing murine CD82 (MK-35). Calnexin is shown as a control for equal loading.

Because the reported observation implicating gp78 in HMGCR regulation was made using a high-speed membrane pellet from cells (Song *et al.*, 2005), we carried out additional experiments in *gp78*$^{-/-}$ MEFs using this approach. Similar results to those using postnuclear supernatants from detergent lysates were obtained; there was no evidence that knockout of gp78 mitigated the sterol-mediated loss of HMGCR (Figure 2E).

A second ubiquitin ligase, TRC8, has also been recently implicated in HMGCR degradation (Jo *et al.*, 2011). These results in SV-589 cells suggest that knockdown of either gp78 or TRC8 with small interfering RNAs (siRNAs) results in partial (50–60%) inhibition of HMGCR degradation, whereas knockdown of both ubiquitin ligases almost completely (90%) abrogates sterol-stimulated degradation of HMGCR. Furthermore, it was reported that gp78 targets TRC8 for degradation such that knockdown of gp78 increases TRC8 protein levels threefold to fourfold, apparently contributing to its overall effect on HMGCR degradation when gp78 expression is diminished. We found no substantial difference in TRC8 levels in *gp78*$^{-/-}$ and WT MEFs, although *gp78*$^{-/-}$ MEFs did exhibit elevated levels of endogenous Insig-1 (Figure 2F). This is consistent with previous reports that gp78 plays an important role in regulating Insig-1 protein levels (Lee *et al.*, 2006; Shmueli *et al.*, 2009).

Taken together, the findings presented thus far lead us to conclude that, in primary MEFs, gp78 is required for the degradation of both endogenous CD82/KAI1 and Insig-1. In contrast, gp78 is dispensable for sterol-stimulated degradation of endogenous HMGCR.

Knockdown of gp78 in Rat-1 cells stabilizes Insig-1 but not HMGCR

The lack of requirement for gp78 in the degradation of HMGCR in MEFs could be due to species differences between MEFs and human SV-589 cells. To begin to evaluate this possibility, we examined the rat fibroblast cell line Rat-1, which we had stably transduced to express doxycycline (Dox)-inducible short hairpin RNAs (shRNAs) that are either unrelated to (control [CTL]) or specific for rat gp78 (1831gp78). Doxycycline treatment reduced the level of gp78 by ~85% in these cells (Figure 3A). Consistent with the data obtained in MEFs and as previously reported (Lee *et al.*, 2006), this decrease in gp78 was accompanied by an increase in the level of stably transfected Myc-tagged Insig-1 without significantly changing the levels of endogenous HMGCR (Figure 3A). To corroborate the effects of gp78 depletion on Insig-1, we directly measured the degradation of Insig-1–Myc by pulse-chase metabolic labeling. Knockdown of gp78 resulted in increased Insig-1–Myc levels and reduced the rate of Insig-1–Myc degradation

Given our results, we sought to verify that the sterol-stimulated decline in HMGCR levels in MEFs, in the complete absence of gp78, is due to ubiquitin-mediated proteasomal degradation. This was confirmed by the finding that sterol-accelerated loss of HMGCR from both *gp78*$^{-/-}$ and WT MEFs was prevented by MG132 (Figure 2D), which inhibits proteasome function (Palombella *et al.*, 1994). In addition, in cells treated with sterols and MG132, ubiquitinated HMGCR accumulated to a similar extent in both WT and gp78$^{-/-}$ cells (Figure 2D).

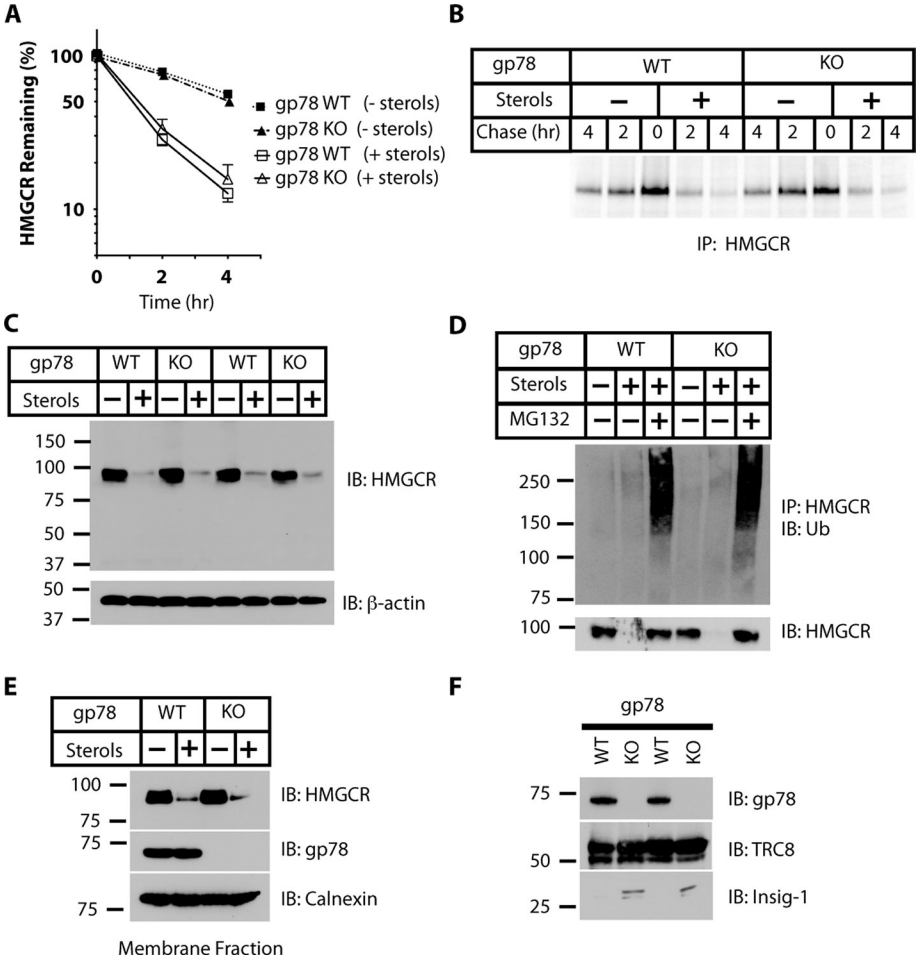

FIGURE 2: gp78 is dispensable for sterol-accelerated degradation of endogenous HMGCR in primary MEFs. (A) gp78 KO MEFs and WT controls were incubated in LPDS medium containing compactin and a low concentration of MVA (medium B; see *Materials and Methods*) for 16–20 h. Cells were metabolically labeled for 30 min with [^{35}S]methionine/cysteine in medium B, followed by chase in medium B, supplemented with excess methionine and cysteine, in the absence or presence of sterols (2 μg/ml 25-HC plus 20 μg/ml cholesterol). Endogenous HMGCR was immunoprecipitated from postnuclear detergent lysates at the indicated time points. Data are from multiple experiments using two sets of paired MEFs ($n = 3$, mean ± SD). (B) Representative autoradiogram from data quantified in A. (C) gp78 KO or WT MEFs were incubated in medium B for 20 h and then treated for 3 h with or without sterols, as in A. Lysates were resolved by SDS–PAGE and immunoblotted (IB) with a mouse monoclonal antibody directed against HMGCR (A9). Shown are samples from two sets of paired MEFs. β-Actin was used as an equal loading control. (D) Cells were allowed to accumulate HMGCR in medium B for 20 h, followed by addition of sterols where indicated, as in A, in the presence or absence of MG132 for 60 min. After lysis, HMGCR was immunoprecipitated (IP) with HMGCR antibodies raised in rabbit and immunoprecipitates were sequentially immunoblotted (IB) with mouse monoclonal antibodies directed against ubiquitin (Ub) and HMGCR. Relative molecular weights are indicated. (E) Same as in C, except that cells were broken mechanically without detergent and membrane fractions were isolated by ultracentrifugation. Membrane fractions were solubilized in SDS sample buffer, resolved by SDS–PAGE, and immunoblotted with mouse monoclonal antibody directed against HMGCR or with anti-gp78 antiserum. Calnexin was used as a control for equal loading. (F) Lysates from gp78 KO or WT MEFs were resolved by SDS–PAGE and immunoblotted with antibodies specific for the indicated proteins. Shown are samples from the two different sets of MEFs.

(Figure 3, B and C). Pulse-chase metabolic labeling was similarly performed to assess endogenous HMGCR degradation (Figure 3, D and E). The marked sterol-stimulated decrease in half-life of HMGCR (30–40 min vs. 10–13 h in the absence of sterols in Rat-1 cells) affords a sensitive readout for conditions that hamper HMGCR degradation. Despite an ~85% decrease in gp78 levels upon induction of shRNA expression (Figure 3E, inset), no decrease in the sterol-accelerated rate of HMGCR degradation was evident. Identical results were obtained in an independent Rat-1–derived cell line, 706gp78, in which a shRNA targeting a different region in the rat gp78 mRNA was stably expressed (Supplemental Figure S1, A and B).

Manipulating gp78 levels in SV-589 cells does not affect sterol-regulated degradation of endogenous HMGCR

The previously reported experiments implicating gp78 as being critical to sterol-stimulated HMGCR ubiquitination and degradation were carried out in SV-589 cells (Song *et al.*, 2005), as were the subsequent experiments implicating TRC8 as a second E3 involved in these processes (Jo *et al.*, 2011). We therefore next assessed the role of gp78 in HMGCR loss in SV-589 cells. In contrast to previous reports, knockdown of gp78 did not prevent the decrease of HMGCR levels in response to sterols in these cells (Figure 4A). The experiments presented in Figure 4A and elsewhere in this study were performed under well-established conditions for analyzing sterol-induced decreases in HMGCR levels (Roitelman and Simoni, 1992; Ravid *et al.*, 2000), using relatively low levels of compactin (MEFs and Rat1 cells, 2 μM; SV-589, 10 μM) to inhibit HMGCR activity and a mixture of 2 μg/ml of 25-HC and 20 μg/ml cholesterol to stimulate HMGCR degradation. However, in the previous studies (Song *et al.*, 2005; Jo *et al.*, 2011), a higher concentration of compactin (50 μM) was used to induce expression of HMGCR, and 25-HC (no cholesterol) and a high concentration of MVA (10 mM) were used to stimulate its degradation. Even using these experimental conditions, we found no discernible effect of gp78 knockdown on the sterol-stimulated decrease in HMGCR levels (Figure 4B). Thus the role of gp78 in HMGCR loss in SV-589 cells similarly could not be verified using this approach. Consistent with ubiquitin-mediated proteasomal degradation, sterol-accelerated loss of endogenous HMGCR was prevented by treatment of cells with MG132 to inhibit the proteasome. Moreover, cells treated with sterols and MG132 accumulated ubiquitinated HMGCR to a similar extent in gp78-depleted cells as in control cells (Figure 4C).

We next performed radioactive pulse-chase experiments to directly measure HMGCR turnover. As with the MEFs and Rat-1 cells, loss of gp78 in SV-589 cells had no effect on the sterol-accelerated degradation of endogenous HMGCR (Figure 4, D and E). This is despite knockdown of gp78 to a similar extent as previously reported (Song *et al.*, 2005; >90%; Supplemental Figure S2). In contrast, knockdown of gp78 was accompanied by

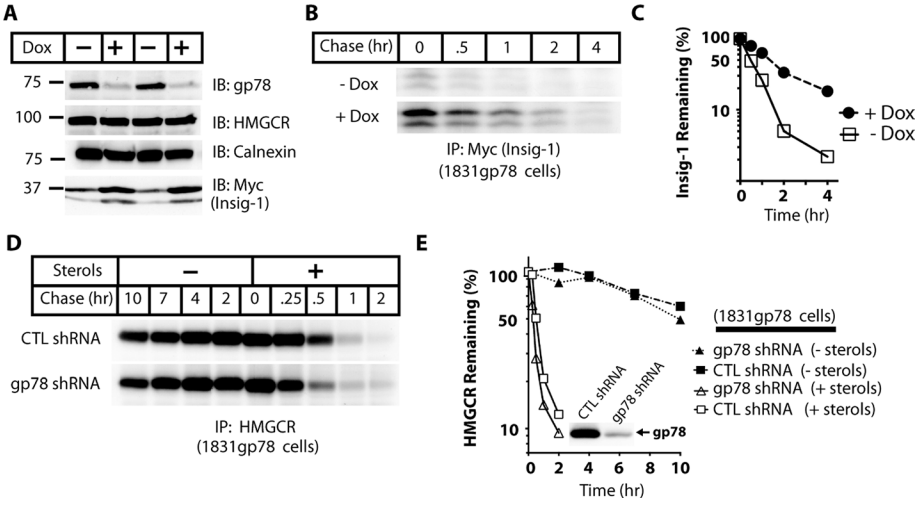

FIGURE 3: gp78 is not required for endogenous HMGCR degradation in Rat-1 cells. (A) Rat-1 cells with a stably integrated doxycycline-inducible gp78 shRNA (1831gp78) were stably transfected with Insig-1–Myc. Cells were treated with doxycycline (Dox) for 48 h to induce shRNA expression and maintained in LPDS medium containing compactin and a low concentration of MVA (medium B) for 16 h before assessment of cell lysates. Samples were immunoblotted (IB) as indicated. Duplicate samples are shown. By densitometry, gp78 levels were estimated to be reduced by ~85% in the doxycycline-treated cells. (B) Cells described in A were treated with or without Dox as in A and incubated in medium B for 16 h. Stability of Insig-1–Myc was assessed by ^{35}S pulse chase and immunoprecipitation with Myc antibodies. (C) Quantification of ^{35}S pulse-chase experiment in B. (D) 1831gp78 or control (CTL) shRNA Rat-1 cells (not transfected with Insig-1–Myc) were treated with Dox and incubated in medium B, as in A. HMGCR degradation was analyzed by ^{35}S pulse chase and immunoprecipitation with HMGCR antibodies. (E) Quantification of ^{35}S pulse-chase experiment shown in D. Inset, relative gp78 levels in this experiment assessed by immunoblotting of cell lysates. gp78 was estimated to be decreased by ~85% upon knockdown. Note: Control (CTL) shRNA samples shown in D and quantified in E were published previously as controls (Wang *et al.*, 2009).

a dramatic increase in the level of transfected Insig-1–Myc and a marked inhibition of its degradation (Figure 4F), in agreement with published findings (Lee *et al.*, 2006).

One potential explanation for the differences between previous publications (Song *et al.*, 2005; Jo *et al.*, 2011) and the findings presented here could lie in the efficiency of gp78 knockdown using different siRNA sequences (see Table 1 for siRNA sequences used in relevant studies). However, we found that each of the siRNAs from all studies, whether used individually or in combination, resulted in a similar (~90%) depletion of gp78 mRNA when transfected under commonly used conditions (Figure 5A). This is also consistent with the reduction of gp78 protein levels seen by Western blotting (Supplemental Figure S2B). Indeed, the striking accumulation and stabilization of transiently expressed Insig-1–Myc in SV-589 cells transfected with gp78 siRNAs underscore the efficiency with which gp78 function had been abrogated in these cells (Figure 4F).

The relationship between gp78, TRC8, and HMGCR was established in SV-589 cells (Jo *et al.*, 2011). To determine whether knockdown of gp78 increases TRC8 levels, potentially compensating in part for the loss of gp78, we transfected SV-589 cells with gp78 siRNAs and TRC8 siRNAs, either individually or together, and evaluated the reduction of endogenous HMGCR levels in response to sterols (Figure 5B). The study implicating TRC8 pointed to the importance of the gp78 siRNA sequence used in observing an effect on HMGCR degradation (Jo *et al.*, 2011). In particular, it used gp78 siRNA sequence S5 (same as gp78A in Jo *et al.*, 2011; see Table 1), which results in the greatest reduction of gp78 expression (although only marginally different from the others in Figure 5A). We therefore used this siRNA sequence to target gp78, in combination with two TRC8 siRNA sequences that we found most efficient in silencing TRC8 expression, to assess their effect on HMGCR levels in response to sterols. There are several findings of note in Figure 5B. First, in comparing lanes 1 and 2 to lanes 3 and 4, there was no discernible increase in TRC8 levels in response to knockdown of gp78 using siRNA sequence S5 either under sterol-depleted or sterol-replete conditions. Second, neither knockdown of gp78 nor that of TRC8 resulted in a discernible effect on sterol-stimulated decrease in endogenous HMGCR levels. Finally, knockdown of gp78 and TRC8 together similarly had no effect on reduction of HMGCR levels in response to sterols.

The marked difference between our findings and those in previous reports, particularly in SV-589 cells, presents a conundrum. However, in reviewing the original publication on gp78 and HMGCR, we noticed that the concentrations of siRNA used were relatively high, ~200 nM (Song *et al.*, 2005), compared with the amount used here (10–20 nM total), which is within a commonly accepted range. To determine whether the different concentrations of siRNA could contribute to the discrepancy in results, we performed additional experiments using a high concentration of siRNAs (Figure 5C). When we reproduced the transfection conditions that were used in Song *et al.* (2005) using at least one siRNA common to both of our studies, we observed a considerable abrogation of the sterol-stimulated loss of HMGCR with the gp78 siRNAs compared with a control siRNA (Figure 5C, compare lanes 1 and 2 to lanes 3 and 4). High levels of siRNA, notably 100 nM or higher, are known to be more likely to exhibit off-target effects, and this can be further accentuated by the use of a single siRNA sequence (Jackson *et al.*, 2003; Semizarov *et al.*, 2003; Persengiev *et al.*, 2004). Consistent with off-target effects, reintroduction of siRNA-resistant gp78 cDNA into these cells, which resulted in overexpression of gp78, failed to reverse the effects of gp78 siRNAs (compare lanes 5 and 6 to lanes 7 and 8). In contrast, overexpression of siRNA-resistant gp78 restores degradation of CD3-δ and KAI1/CD82 after knocking down endogenous gp78 with 10 nM siRNA (Tsai *et al.*, 2007). There may be other factors that contribute to the differences between our findings and previous reports using SV-589 cells to assess the role of gp78 in sterol-accelerated loss of HMGCR. However, the inability of gp78 overexpression to restore sterol-stimulated HMGCR degradation after transfection with high concentrations of siRNA raises the possibility that off-target effects, due to high levels of a particular gp78 siRNA, may be an important contributing factor.

DISCUSSION

The ER ubiquitin ligases gp78 and TRC8 are important regulators of Insig-1 and of SREBP precursors, respectively (Lee *et al.*, 2006, 2010; Irisawa *et al.*, 2009). Both ligases interact with key components of the sterol regulatory apparatus, including the Insig proteins, SCAP, and the inactive precursor forms of SREBPs in the ER. These ligases

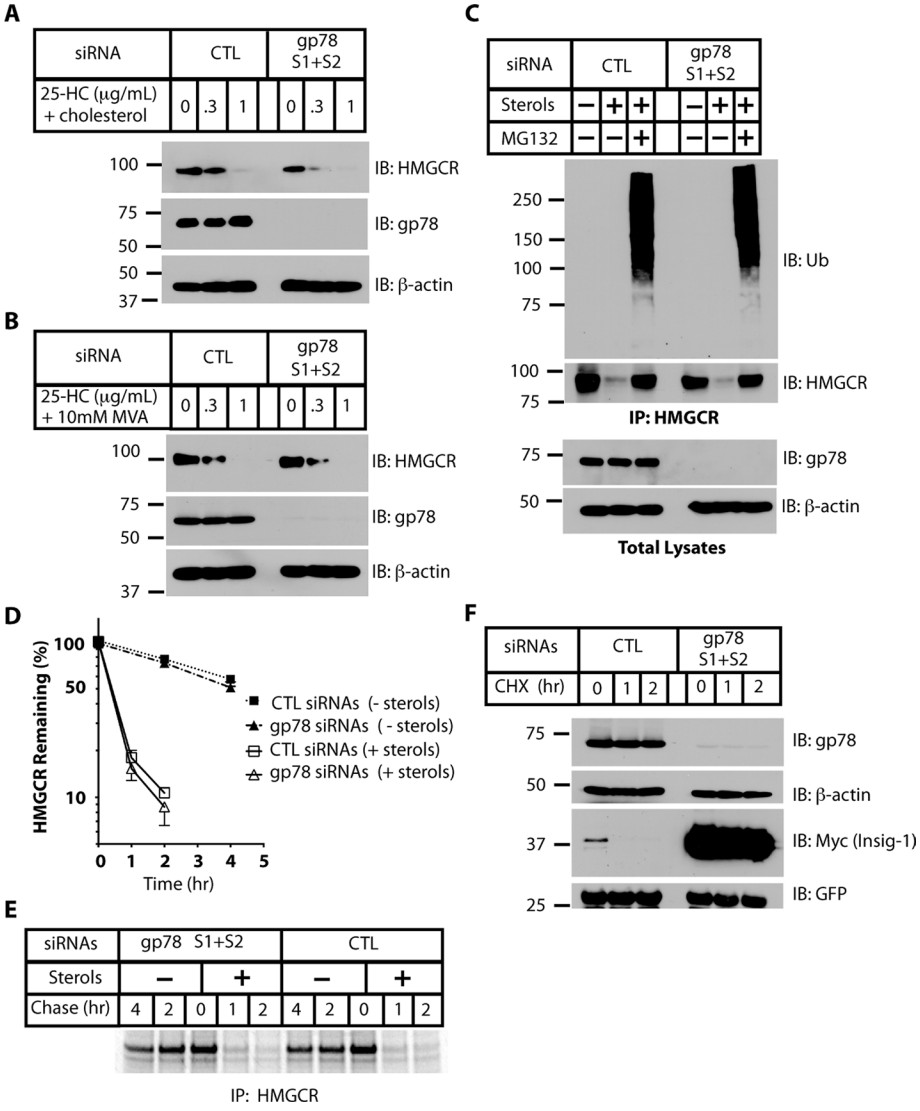

FIGURE 4: gp78 is dispensable for sterol-stimulated degradation of endogenous HMGCR in SV-589 cells. (A) SV-589 cells were transfected with control (CTL) or gp78 siRNAs (see *Materials and Methods* and Table 1 for siRNA sequences). After 40 h, cells were allowed to accumulate HMGCR in LPDS media containing compactin and a low concentration of MVA (medium B; see *Materials and Methods*) for 20 h, followed by 3 h with or without the indicated concentrations of 25-HC and 10-fold more cholesterol. Cell lysates were processed for immunoblotting (IB) as indicated. β-Actin served as an equal loading control. (B) Cells transfected as in A were allowed to accumulate HMGCR in medium B with an increased concentration of compactin (50 μM) for 20 h. Mevalonate at 10 mM and the indicated concentrations of 25-HC (without cholesterol) were then added. After 4 h, cells were lysed, and levels of HMGCR, gp78, and β-actin were assessed by immunoblotting. (C) Cells were transfected with control or gp78 siRNAs and then allowed to accumulate HMGCR, as in A. Cells were treated for 60 min with sterols in the presence or absence of MG132, and cell lysates were processed for immunoprecipitation (IP) with rabbit HMGCR antisera, followed by immunoblotting (IB) with mouse monoclonal antibodies recognizing ubiquitin (Ub) and HMGCR. Cell lysates were probed for gp78 to assess its knockdown. (D) Cells were transfected and allowed to accumulate HMGCR, as in A. The ^{35}S pulse-chase analyses were carried out as in Figure 2A ($n = 3$, mean ± SD). See Supplemental Figure S2 for gp78 levels. (E) Representative autoradiogram from data quantified in D. (F) Cells transfected with siRNAs, as in A, were transfected after 18 h with Insig-1–Myc and with GFP as a control for transfection efficiency. Cells were cultured for an additional 30 h and then treated with 50 μg/ml cycloheximide (CHX) to inhibit protein synthesis while cultured in complete medium (no sterol manipulation). The degradation of Insig-1–Myc was monitored by immunoblotting.

are therefore potentially critical for regulating transcription of HMGCR, as well as nearly all other genes in the cholesterol biosynthetic and uptake pathways. However, the proposed specific role of these E3s in modulating HMGCR stability has yet to be firmly established. With Insig-1 (Lee *et al.*, 2006) and CD82/KAI1 (Tsai *et al.*, 2007) as positive controls, using fibroblast cells from three different species, we found no role for gp78 in the sterol-stimulated degradation of HMGCR, as assessed both by quantitative pulse-chase metabolic labeling and by the decline in its total level. Laboratory-specific "environmental effects" cannot account for our inability to observe a role for gp78, as the experiments in Rat-1 cells were carried out in a different laboratory using different media and sera from those in MEFs and SV-589 cells, the latter being the cell line in which gp78 had been implicated in the regulation of HMGCR (Song *et al.*, 2005; Jo *et al.*, 2011). Furthermore, in contrast to published results, we did not observe an increase in TRC8 in response to gp78 knockdown, even when the most effective siRNA sequence reported (Song *et al.*, 2005; Jo *et al.*, 2011) was used. Moreover, we see no evidence of a role for TRC8 in the degradation of HMGCR when it is knocked down either by itself or together with gp78. A similar lack of effect of TRC8 knockdown on HMGCR stability and ubiquitination was seen in HEK293 cells (G.S.L. and J.R., unpublished observations). Overall, it is clear that sterol-accelerated degradation of HMGCR via the ubiquitin-proteasome system can occur independently of these ubiquitin ligases.

The regulation of enzymes involved in cholesterol metabolism is clearly complex, with intricate feedback loops that are subject to influence by extracellular factors and genetic variability, all of which are difficult to assess. Given this, how can we begin to reconcile the differences between our results and those previously published (Song *et al.*, 2005; Jo *et al.*, 2011)? Because most of the data were obtained through siRNA-mediated knockdown of the ligases in question, one potential difference could result from the combination and amount of siRNA used in the transfection. In the work of Song *et al.* (2005), 10- to 20-fold higher concentrations of individual siRNAs were used than those used here. Such concentrations (100 nM or greater) are more likely to cause off-target effects, which can be further accentuated when a single siRNA sequence is used (Jackson *et al.*, 2003; Semizarov *et al.*, 2003; Persengiev *et al.*, 2004). Indeed, we observed a significant inhibition of HMGCR degradation in cells transfected with a high concentration of gp78 siRNA that could not be relieved by reexpression of siRNA-resistant gp78. Thus off-target effects derived from the use of high concentrations of siRNAs may account for some of the

S1:	UGCACACCUUGGCUUUCAU (638–656)	gp78 S1 in Tsai *et al.*, 2007; gp78B in Jo *et al.*, 2011
S2:	GUUUGGCCCUCUUCGAGUG (318–336)	gp78 S2 in Tsai *et al.*, 2007; gp78C in Jo *et al.*, 2011
S3:	GCUCAUCCAGUGUAUUGUG (300–318)	Similar to gp78A in Song *et al.*, 2005, which includes 298–299 (AA)
S4:	GUGAUGCACACCACCAACA (1318–1336)	
S5:	CAUGCAGAAUGUCUCUUAA (1130–1148)	gp78A in Jo *et al.*, 2011

TABLE 1: gp78 sequences used for SV-589 cells.

discrepancies between our data and those reported (Song *et al.*, 2005; Jo *et al.*, 2011).

From an in vivo and physiological viewpoint, the stabilization and concomitant accumulation of Insig-1 by loss of gp78 expression might be predicted to cause inhibition of gene expression of HMGCR, and likely all other enzymes of the mevalonate pathway, through Insig-1–mediated retention of the SCAP–SREBP complex in the ER (Yang *et al.*, 2002; Engelking *et al.*, 2004). This effect may be exaggerated in the liver, a major cholesterol-synthesizing and -exporting organ, and could potentially lead to an intracellular shortage of mevalonate-derived metabolites, especially nonsterols that are critical for sterol-stimulated degradation of HMGCR (Nakanishi *et al.*, 1988; Roitelman and Simoni, 1992; Leichner *et al.*, 2011). The net outcome could be an attenuation of sterol-accelerated degradation of HMGCR. This view is consistent with the recent study by Song and colleagues, who examined mice in which gp78 is specifically ablated in the liver (Liu *et al.*, 2012). The major effect of gp78 loss is inhibition of SREBP processing and increased levels of Insig-1 and Insig-2. These recent findings are in agreement with our data regarding Insig-1 and support earlier reports on the antilipogenic effects of Insig(s) overexpression in the liver (Takaishi *et al.*, 2004; Engelking *et al.*, 2004). However, in the *gp78*$^{-/-}$ livers, HMGCR levels are also increased, and in isolated *gp78*$^{-/-}$ hepatocytes there is a marked diminution in the dose-dependent loss of HMGCR in response to sterols. Despite this increase in HMGCR protein, cholesterol synthesis—a measure of the flux of intermediates through the mevalonate pathway—is actually decreased in *gp78*$^{-/-}$ hepatocytes (Liu *et al.*, 2012). This result is reminiscent of the opposing effects of statins on HMGCR levels and actual cholesterol synthesis. Thus, although these observations were interpreted as a loss of gp78-mediated HMGCR degradation (Liu *et al.*, 2012), the issue of direct targeting of HMGCR for degradation by gp78 remains to be rigorously addressed in *gp78*$^{-/-}$ hepatocytes.

Beyond this, there are several points to be considered regarding data obtained with the different gp78 knockouts. First, the genomic deletion used by Song and coworkers is different from the one we used here. It is well documented that, for reasons that are not always evident, different gene-targeting approaches may lead to different results and that unanticipated functions due to products of interrupted transcripts must be excluded (e.g., Yamaguchi *et al.*, 2005;

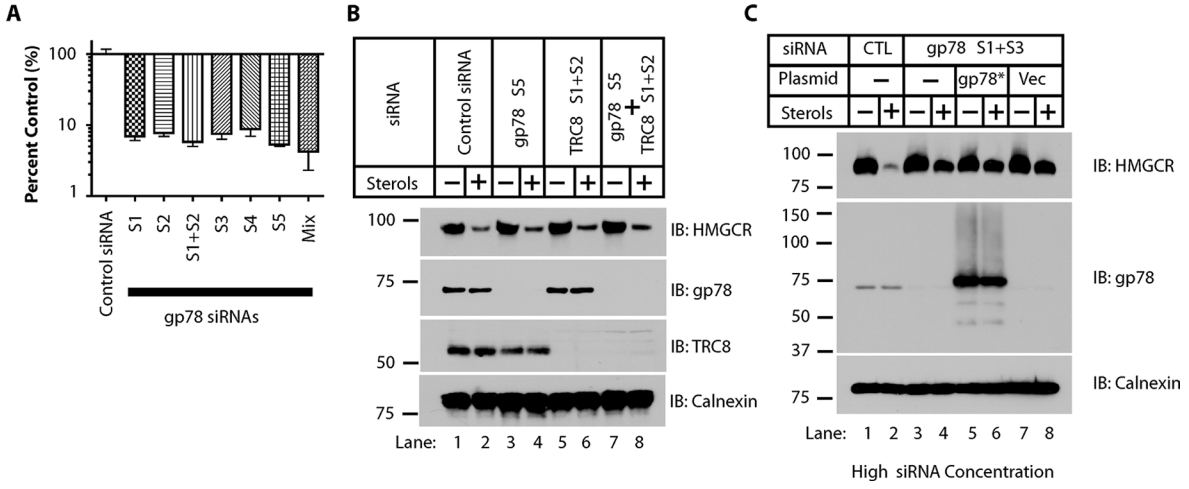

FIGURE 5: Effect of gp78 siRNA concentration on endogenous HMGCR levels in SV-589 cells. (A) SV-589 cells were transfected with individual or combinations of gp78 siRNAs described in Table 1. In each condition a total of 10 nM siRNA was used. "Mix" indicates transfection with equal amount of all five siRNAs. After 48 h, RNA was extracted and gp78 mRNA was measured by real-time PCR. Data shown are normalized to β-actin mRNA ($n = 3$, mean ± SD). (B) SV-589 cells were transfected with gp78 siRNA sequence S5, which gives a marginally more efficient knockdown of gp78 mRNA than the other four, in combination with TRC8 siRNAs. Total siRNA concentration is 20 nM (10 nM for each gene product, with 10 nM control siRNA when mRNAs are knocked down individually). Cells were allowed to accumulate HMGCR in medium B for 20 h, followed by a 3 h incubation with or without sterols. Cells were lysed and processed for immunoblotting (IB) as indicated. Calnexin is used as a control for equal loading. (C) SV-589 cells were transfected with 200 nM total of control (CTL) or gp78 siRNAs. After 8 h, cells were transfected with vector or siRNA-resistant gp78 (gp78*). Cells were allowed to accumulate HMGCR in medium B for 20 h, followed by a 3 h incubation with or without sterols. Cells were lysed and processed for immunoblotting with the indicated antibodies. Calnexin serves as an equal loading control.

Cheng *et al.*, 2007; Mittelstadt *et al.*, 2012). We deleted exons 7 and 8 of the *gp78* gene, whereas Song and colleagues deleted exons 5–8. These different deletions could result in the expression of different N-terminal truncations of gp78 that could have unanticipated effects. To test this, we generated an antibody against the N-terminus of gp78 (amino acids [aa] 33–54) to ensure that truncated gp78 is not expressed in the knockout described here, ruling out aberrancies that might be created by the generation of a partial gene product (Figure 1D). In addition, as the region deleted by targeted recombination increases in size, the probability of unanticipated effects on other genes increases. Careful analysis in the future should help to clarify this issue. Second, whereas the recently published work was carried out in mice that were primarily of C57BL/6J background, our paired MEFs were derived from mice of a mixed background. Genetic background can markedly affect the phenotype observed when a gene is inactivated if genetic modifiers present in the different strains regulate the process being studied (Sanford *et al.*, 2001). Finally, our studies were based on primary fibroblasts (MEFs); fibroblasts are the lineage in which the gp78 relationship was first shown by DeBose-Boyd, Song, and coworkers. The recent study used primary hepatocytes (Liu *et al.*, 2012). Different cell types could certainly contribute to differences in results. Indeed, loss of gp78 results in massive accumulation of Insig-2 in hepatocytes (Liu *et al.*, 2012), in contrast to earlier findings in CHO and SV-589 cells, where Insig-2 was found to be a fairly stable protein (Lee and Ye, 2004) that does not associate well with gp78 and was concluded to likely not be regulated by this E3 (Lee *et al.*, 2006). Moreover, Insig-1 accumulated only slightly in the $gp78^{-/-}$ liver (Liu *et al.*, 2012), despite being a bona fide substrate for gp78, as reported previously (Lee *et al.*, 2006) and shown here.

gp78 is a critical ubiquitin ligase that is implicated in the regulation of cholesterol homeostasis through its effects on the stability of Insig-1 and possibly Insig-2. However, exactly what role it plays in targeting HMGCR for degradation and how that role might vary in different cell types or conditions clearly require further assessment. This is especially important as consideration is given to the clinical utility of manipulating the activity of this important ubiquitin ligase.

MATERIALS AND METHODS

Reagents

MG132 and *N*-acetyl-leucyl-leucyl-norleucinal (ALLN) were from Calbiochem (La Jolla, CA) or Sigma-Aldrich (St. Louis, MO); Igepal CA-630, which is chemically indistinguishable from NP-40, was from Sigma-Aldrich. Geneticin (G-418) was from Invitrogen (Carlsbad, CA); puromycin was from MP Biomedicals (Solon, OH). Protein A–Sepharose was from RepliGen (Waltham, MA); protein G–Sepharose was from GE Healthcare Life Sciences (Piscataway, NJ). ^{35}S-labeling mix was from PerkinElmer Life (Waltham, MA), Analytical Sciences (Woodbridge, Canada), or MP Biomedicals. Visualization of immunoblots was carried out by enhanced chemiluminescence (ECL) using SuperSignal West Pico Chemiluminescent Substrate from Thermo Scientific Pierce (Rockford, IL). 25-Hydroxycholesterol (5-cholesten-3β; 25-diol; 25-HC) and cholesterol were from Steraloids (Newport, RI). All other reagents, except where noted, were from Sigma-Aldrich. Stock sterol solutions were prepared in 100% ethanol at a 200× final concentration. Unless otherwise indicated, sterols were added to media to final concentrations of 2 μg/ml 25-HC + 20 μg/ml cholesterol. Mevalonolactone (Fluka, Buchs, Switzerland) was converted to sodium mevalonate by base hydrolysis. Fetal bovine lipoprotein–deficient serum (LPDS; $d > 1.25$) was prepared by ultracentrifugation, as described (Goldstein *et al.*, 1983).

Antibodies

Affinity-purified rabbit polyclonal rat gp78 antibody (aa 624–642; used for all experiments with Rat-1 cells; Pearce *et al.*, 2007), affinity-purified rabbit polyclonal mouse/human gp78 antibody (gp78 Ab2; used for all experiments with mouse or human gp78 except Figure 1D; Tsai *et al.*, 2007), rabbit polyclonal HMGCR antibody (Roitelman *et al.*, 1992), and rabbit polyclonal calnexin antibody (Leichner *et al.*, 2009) have been previously described. Mouse monoclonal HMGCR antibody (A9; Liscum *et al.*, 1983b) was obtained from the American Type Culture Collection (Manassas, VA) and was prepared in mice as ascites fluid or harvested from conditioned medium. Polyclonal antibody (gp78 Ab3) directed against a transmembrane region of mouse gp78 encoded by exon 1 (aa 33–54) used in Figure 1D was generated in rabbit and affinity purified. Rabbit polyclonal antibody recognizing murine CD82/KAI1 (MK-35) was a generous gift from Mary Custer (National Cancer Institute, Frederick, MD) and J. Carl Barrett (AstraZeneca, Wilmington, DE; Custer *et al.*, 2006). Mouse monoclonal antibody recognizing β-actin was from Sigma-Aldrich. Mouse monoclonal Myc epitope-tag antibody 9E10 was prepared from culture supernatant. Antibodies recognizing TRC8 (aa 576–664; H-89), green fluorescent protein (B-2), and ubiquitin (P4D1) were from Santa Cruz Biotechnology (Santa Cruz, CA). Antibody recognizing Insig-1 (ab70784) was from Abcam (Cambridge, MA). Rabbit polyclonal HMGCR antibody was used for all immunoprecipitations, and mouse monoclonal HMGCR antibody (A9) was used for immunoblotting. Secondary antibodies directed against rabbit or mouse immunoglobulin G were from GE Healthcare Life Sciences or Jackson Immunoresearch Laboratories (West Grove, PA).

Cells

A floxed gp78 allele was created by introducing loxP sites into the intron between exons 8 and 9 and a selectable neocassette (G418 resistance) surrounded by loxP and FRT sites between exons 6 and 7, using recombineering methods (Court *et al.*, 2003; Figure 1A). Stem cells (129/SvJ) were screened for recombination by long-range PCR and Southern blot analysis and used to generate chimeric mice. After germline transmission, the mice were crossed to C57BL/6J-expressing, transgenic β-actin–driven Cre to generate a deletion mutant allele, eliminating exons 7 and 8, encoding part of the most C-terminal transmembrane domain and half of the RING finger, respectively. Heterozygous mice ($gp78^{+/-}$; Cre^{-}) were backcrossed to C57BL/6J mice for five generations for this study. Primary MEFs were prepared from somites of E12.5 embryos derived from mating $gp78^{+/-} \times gp78^{+/-}$ mice. Two sets of WT and knockout MEFs were derived; each set was from a different pregnancy. The tails were removed from the embryos for genotyping by PCR (forward primer, CCCAGCACCATAGAAAGGAAA; WT reverse primer, ACATGGCTCTTCCGCCTAGGCA; KO reverse primer, CCATGTGGCTCACTCAGCCAG), and complete loss of the protein in the KO MEFs was confirmed by immunoblots with gp78 antibodies. MEFs were maintained in DMEM containing 10% (vol/vol) fetal bovine serum (FBS), 2 mM glutamine, 100 U/ml penicillin, and 100 μg/ml streptomycin in a 3% O_2 incubator. Because deletion of exons 7 and 8 could potentially result in translation of a gp78 fragment that terminates after exon 6 (amid the most C-terminal transmembrane domain), MEFs were assessed for and found to lack any evidence of a truncated gp78 protein (Figure 1D). SV-589 cells (Song *et al.*, 2005) were a generous gift from Jin Ye (University of Texas Southwestern Medical Center, Dallas, TX). Cells were maintained in DMEM supplemented with 10% (vol/vol) heat-inactivated FBS, 2 mM glutamine, 100 U/ml penicillin, and 100 μg/ml streptomycin (medium A). For

Rat-1 cells, medium A also contained 10 mM Na 4-(2-hydroxyethyl)-1-piperazineethanesulfonic acid, pH 7.4.

To generate Rat-1 cells expressing inducible shRNAs for gp78, retroviruses containing shRNA-encoding 6OH1O-pSUPER.retro.puro vectors (Pearce *et al.*, 2007) were generated in HEK293T cells and titered, and Rat-1 cells stably expressing tTS (a fusion protein of the Tet repressor) were transduced twice as described (Pearce *et al.*, 2009). shRNA expression was induced by treating virally transduced cells with 1 μg/ml doxycycline for 48 h, followed by selection of shRNA-expressing cells with 1 μg/ml doxycycline plus 2.5 μg/ml puromycin for an additional 24–48 h. Cell lines expressed shRNAs that included 19 nucleotides beginning with base 706 (706gp78) or 1831 (1831gp78) of the rat gp78-coding region (accession no. XM_341644) or consisting of a random sequence with no homology to any known mammalian mRNA sequences (ACTGTCACAAGTACCTACA; "CTL"). Cells were maintained in medium A with 250 μg/ml G-418 sulfate. Experiments were carried out using 1831gp78 and CTL cells, and ^{35}S-pulse chase analysis was confirmed using 706gp78 (Supplemental Figure S1). To generate inducible cell lines stably expressing Insig-1–Myc, transduced Rat-1 cells were transfected with Insig-1–Myc plasmid (see later description) using jetPEI reagent (Polyplus-transfection, New York, NY), according to the manufacturer's procedure. Transfectants were selected in 400 μg/ml hygromycin, and resistant colonies were pooled and expanded. Cells were maintained in medium A with 250 μg/ml G-418 and 200 μg/ml hygromycin. Cells were prepared for experiments involving sterol manipulation by incubating for 16–20 h in DMEM supplemented with 10% (vol/vol) LPDS, 100 μM sodium mevalonate, and compactin (medium B) before initiation of experiments. For all MEF and Rat-1 experiments, 2 μM compactin was used. For SV-589 experiments, 10 μM compactin was used, except where indicated (Figure 4B). For Rat-1–derived cells this was preceded by treatment for 48 h in medium A supplemented with or without 1 μg/ml doxycycline and 2.5 μg/ml puromycin to induce shRNA expression.

Plasmids and transfections

Plasmid encoding Insig-1–Myc (Yang *et al.*, 2002), a gift from Joseph Goldstein (University of Texas Southwestern Medical Center), was used as is or after subcloning into pcDNA3.1/hyg vector (Clontech, Mountain View, CA), as described (Leichner *et al.*, 2009). siRNAs directed against human gp78 are as follows: siRNA-1, UGCACACCUUGGCUUUCAU (638–656); siRNA-2, GUUUGGCCCUCUUCGAGUG (318–336); siRNA-3, GCUCAUCCAGUGUAUUGUG (300–318); siRNA-4, GUGAUGCACACCACCAACA (1318–1336); and siRNA-5, CAUGCAGAAUGUCUCUUAA (1130–1148) (see Table 1). siRNAs targeting TRC8 are as follows: siRNA-1, CAGAGAGACTTTACTGTTTTT (522–540); and siRNA-2, GGGAAAAGCTTGACGATTA (1361–1379). To generate a siRNA-resistant gp78 (gp78*), silent mutations were introduced by site-directed mutagenesis (forward primers: P1, GCTACACCCACGGAATGCATACGCTAGCCTTTATGGCTGCAGAGTCT; and P2, TTGATGTTGGTGGCTAAATTGATACAGTGCATCGTCTTTGGCCCTCTTCGA). Transfections of SV-589 with siRNAs and Insig-1–Myc were carried out using HiPerfect (Qiagen, Valencia, CA) and Lipofectamine 2000 (Invitrogen), respectively, with the exception of Figure 5C, involving the use of a high concentration of siRNAs. For experiments involving a high concentration of siRNAs, we followed the transfection procedure as described (Song *et al.*, 2005), using Oligofectamine (Invitrogen) and 200 nM siRNA. In experiments involving sterol manipulation, siRNA transfection preceded incubation in medium B by 40 h. For experiments involving siRNA and expression of Insig-1–Myc, siRNA transfection preceded plasmid transfection by 18 h unless otherwise indicated. Experiments were carried out 30 h after plasmid transfection.

Pulse-chase metabolic labeling

Pulse-chase experiments were carried out in cells preincubated for 16–20 h in medium B, essentially as described (Roitelman *et al.*, 1992). Briefly, cells were starved for amino acids by 1 h of incubation in medium B lacking methionine and cysteine. The cells were pulse labeled for 30–45 min with 300 μCi/ml of ^{35}S protein–labeling mix in medium B lacking methionine and cysteine and then chased in complete medium B in the absence or presence of sterols and with excess unlabeled methionine and cysteine. Unless otherwise indicated, final concentrations of sterols in the chase were 2 μg/ml 25-HC and 20 μg/ml cholesterol. At the indicated time points the cells were washed in phosphate-buffered saline (PBS). Cells were lysed in PBS containing 1% (vol/vol) Triton X-100 for MEFs and SV-589 cells or 1% (vol/vol) Igepal CA-630 for Rat-1 cells. All lysis buffers included 1% (wt/vol) sodium deoxycholate, 5 mM EDTA, 5 mM ethylene glycol tetraacetic acid, 2 mM phenylmethysulfonyl fluoride, 100 μM leupeptin, and 35 μM ALLN. Lysates were centrifuged at 20,000 × *g* for 30 min, and rabbit antisera targeting the membrane regions of HMGCR (or anti–c-Myc in the case of Insig-1–Myc) were added to the clarified postnuclear supernatants, followed by protein A or protein G–Sepharose beads. Immunoprecipitates were extensively washed and resolved by SDS–PAGE under reducing conditions. Quantification of the Rat-1 experiments was carried out after impregnating the fixed gels in sodium salicylate, followed by exposure to x-ray film at –80°C and densitometric scanning of films with exposures that were within a linear range. For experiments in MEFs and SV-589, quantification was performed using Storm Phosphorimager and Image Quant software (GE Healthcare Life Sciences).

Assessment of protein levels and ubiquitination

For all experiments except for Figure 2E (see later description), cells were lysed in detergent-containing buffer and insoluble material removed by centrifugation as described for pulse-chase experiments. Postnuclear detergent-soluble lysates were made 1× in reducing SDS–PAGE sample buffer and resolved by SDS–PAGE under reducing conditions, followed by transfer to nitrocellulose or polyvinylidene fluoride membranes and immunoblotting with the indicated antibodies. For assessment of ubiquitination, cells were treated with 50 μM MG132 with or without sterols, as indicated. Cells were lysed as described, except that 10 mM iodoacetamide was included in the lysis buffer to inactivate deubiquitinating enzymes. HMGCR was immunoprecipitated from equal amounts of postnuclear supernatant with rabbit anti-HMGCR membrane region antiserum. After SDS–PAGE under reducing conditions and transfer, membranes were probed for ubiquitin (P4D1) and HMGCR (A9) as indicated.

Isolation of membrane fraction

Subcellular fractionation was performed as described (Chen *et al.*, 2006). Briefly, cells were resuspended in homogenization buffer (0.25 M sucrose/10 mM triethanolamine/1 mM EDTA, pH 7.4, supplemented with protease inhibitor cocktail [Roche, Indianapolis, IN] and 20 μM MG132) for 10 min at 4°C, followed by 15 passages through a 27-gauge needle. The products were subject to two sequential 5-min 1000 × *g* spins at 4°C to remove unbroken cells and nuclei. Supernatants from the 1000 × *g* spin were subject to 100,000 × *g* for 1 h at 4°C to pellet the membrane fraction.

Quantitative PCR

Total RNA was extracted from cells using TRIzol reagent (Invitrogen) and reverse transcribed into cDNA using SuperScript III First-Strand Synthesis System for RT-PCR (Invitrogen) according to the manufacturer's instructions. Quantitative PCR was performed in iCycler using iQ SYBR Green Supermix (Bio-Rad, Hercules, CA) with QuantiTect primers (gp78, QT00036085; Qiagen) in a 20-µl volume. Thermal cycling was carried out with a 5-min denaturation step at 95°C, followed by 40 three-step cycles: 15 s at 95°C, 30 s at 60°C, and 30 s at 72°C. Amplification data were collected by iCycler collection software, version 3.1, and analyzed by $\Delta\Delta Ct$ method with β-actin as the internal control (QuantiTect primers, QT00036085).

ACKNOWLEDGMENTS

We thank Lino Tessarollo and Shyam K. Sharan (National Cancer Institute) for invaluable advice and assistance in generating mice expressing a conditional gp78-knockout allele, Joseph Goldstein and Jin Ye (University of Texas Southwestern Medical Center) for gifts of invaluable reagents, Amy James (National Cancer Institute) for excellent animal technical service, Mei Yang (National Cancer Institute) for assistance with genotyping and MEF generation, and Acong Yang (National Cancer Institute) for assistance with quantitative PCR. We are also grateful to Shoshana Bar-Nun, Stanley Lipkowitz, Meredith Metzger, and Daniel Stringer for useful discussions and critical reading of the manuscript. This work was supported by the National Cancer Institute, National Institutes of Health Intramural Research Program (Y.C.T., G.L.W., A.M.W.), fellowships from the Amalia Biron-Cegla Fund and the Crown Family Foundation (G.S.L.), National Institutes of Health Grant DK49194 (R.J.H.W.), and a predoctoral fellowship from the PhRMA Foundation (M.M.P.).

REFERENCES

Brown MS, Faust JR, Goldstein JL, Kaneko I, Endo A (1978). Induction of 3-hydroxy-3-methylglutaryl coenzyme A reductase activity in human fibroblasts incubated with compactin (ML-236B), a competitive inhibitor of the reductase. J Biol Chem 253, 1121–1128.

Brown MS, Goldstein JL (1980). Multivalent feedback regulation of HMG CoA reductase, a control mechanism coordinating isoprenoid synthesis and cell growth. J Lipid Res 21, 505–517.

Chen B, Mariano J, Tsai YC, Chan AH, Cohen M, Weissman AM (2006). The activity of a human endoplasmic reticulum-associated degradation E3, gp78, requires its Cue domain, RING finger, and an E2-binding site. Proc Natl Acad Sci USA 103, 341–346.

Cheng J, Kang X, Zhang S, Yeh ET (2007). SUMO-specific protease 1 is essential for stabilization of HIF1alpha during hypoxia. Cell 131, 584–595.

Chun KT, Bar-Nun S, Simoni RD (1990). The regulated degradation of 3-hydroxy-3-methylglutaryl-CoA reductase requires a short-lived protein and occurs in the endoplasmic reticulum. J Biol Chem 265, 22004–22010.

Court DL, Swaminathan S, Yu D, Wilson H, Baker T, Bubunenko M, Sawitzke J, Sharan SK (2003). Mini-lambda: a tractable system for chromosome and BAC engineering. Gene 315, 63–69.

Custer MC, Risinger JI, Hoover S, Simpson RM, Patterson T, Barrett JC (2006). Characterization of an antibody that can detect the Kai1/CD82 murine metastasis suppressor. Prostate 66, 567–577.

Edwards PA, Lan SF, Fogelman AM (1983). Alterations in the rates of synthesis and degradation of rat liver 3-hydroxy-3-methylglutaryl coenzyme A reductase produced by cholestyramine and mevinolin. J Biol Chem 258, 10219–10222.

Engelking LJ, Kuriyama H, Hammer RE, Horton JD, Brown MS, Goldstein JL, Liang G (2004). Overexpression of Insig-1 in the livers of transgenic mice inhibits SREBP processing and reduces insulin-stimulated lipogenesis. J Clin Invest 113, 1168–1175.

Faust JR, Luskey KL, Chin DJ, Goldstein JL, Brown MS (1982). Regulation of synthesis and degradation of 3-hydroxy-3-methylglutaryl-coenzyme A reductase by low density lipoprotein and 25-hydroxycholesterol in UT-1 cells. Proc Natl Acad Sci USA 79, 5205–5209.

Goldstein JL, Basu SK, Brown MS (1983). Receptor-mediated endocytosis of low-density lipoprotein in cultured cells. Methods Enzymol 98, 241–260.

Goldstein JL, Brown MS (1990). Regulation of the mevalonate pathway. Nature 343, 425–430.

Goldstein JL, DeBose-Boyd RA, Brown MS (2006). Protein sensors for membrane sterols. Cell 124, 35–46.

Hampton RY, Gardner RG, Rine J (1996). Role of 26S proteasome and HRD genes in the degradation of 3-hydroxy-3-methylglutaryl-CoA reductase, an integral endoplasmic reticulum membrane protein. Mol Biol Cell 7, 2029–2044.

Hirsch C, Jarosch E, Sommer T, Wolf DH (2004). Endoplasmic reticulum-associated protein degradation—one model fits all? Biochim Biophys Acta 1695, 215–223.

Irisawa M, Inoue J, Ozawa N, Mori K, Sato R (2009). The sterol-sensing endoplasmic reticulum (ER) membrane protein TRC8 hampers ER to Golgi transport of sterol regulatory element-binding protein-2 (SREBP-2)/SREBP cleavage-activated protein and reduces SREBP-2 cleavage. J Biol Chem 284, 28995–29004.

Jackson AL, Bartz SR, Schelter J, Kobayashi SV, Burchard J, Mao M, Li B, Cavet G, Linsley PS (2003). Expression profiling reveals off-target gene regulation by RNAi. Nat Biotechnol 21, 635–637.

Jo Y, Debose-Boyd RA (2010). Control of cholesterol synthesis through regulated ER-associated degradation of HMG CoA reductase. Crit Rev Biochem Mol Biol 45, 185–198.

Jo Y, Lee PC, Sguigna PV, DeBose-Boyd RA (2011). Sterol-induced degradation of HMG CoA reductase depends on interplay of two Insigs and two ubiquitin ligases, gp78 and Trc8. Proc Natl Acad Sci USA 108, 20503–20508.

Kaneko I, Hazama-Shimada Y, Endo A (1978). Inhibitory effects on lipid metabolism in cultured cells of ML-236B, a potent inhibitor of 3-hydroxy-3-methylglutaryl-coenzyme-A reductase. Eur J Biochem 87, 313–321.

Kikkert M, Doolman R, Dai M, Avner R, Hassink G, van Voorden S, Thanedar S, Roitelman J, Chau V, Wiertz E (2004). Human HRD1 is an E3 ubiquitin ligase involved in degradation of proteins from the endoplasmic reticulum. J Biol Chem 279, 3525–3534.

Kostova Z, Tsai YC, Weissman AM (2007). Ubiquitin ligases, critical mediators of endoplasmic reticulum-associated degradation. Semin Cell Dev Biol 18, 770–779.

Lee JN, Song B, DeBose-Boyd RA, Ye J (2006). Sterol-regulated degradation of Insig-1 mediated by the membrane-bound ubiquitin ligase gp78. J Biol Chem 281, 39308–39315.

Lee JN, Ye J (2004). Proteolytic activation of sterol regulatory element-binding protein induced by cellular stress through depletion of Insig-1. J Biol Chem 279, 45257–45265.

Lee JP, Brauweiler A, Rudolph M, Hooper JE, Drabkin HA, Gemmill RM (2010). The TRC8 ubiquitin ligase is sterol regulated and interacts with lipid and protein biosynthetic pathways. Mol Cancer Res 8, 93–106.

Leichner GS, Avner R, Harats D, Roitelman J (2009). Dislocation of HMG-CoA reductase and Insig-1, two polytopic endoplasmic reticulum proteins, en route to proteasomal degradation. Mol Biol Cell 20, 3330–3341.

Leichner GS, Avner R, Harats D, Roitelman J (2011). Metabolically regulated endoplasmic reticulum-associated degradation of 3-hydroxy-3-methylglutaryl-CoA reductase: evidence for requirement of a geranylgeranylated protein. J Biol Chem 286, 32150–32161.

Liscum L, Cummings RD, Anderson RG, DeMartino GN, Goldstein JL, Brown MS (1983a). 3-Hydroxy-3-methylglutaryl-CoA reductase: a transmembrane glycoprotein of the endoplasmic reticulum with N-linked "high-mannose" oligosaccharides. Proc Natl Acad Sci USA 80, 7165–7169.

Liscum L, Luskey KL, Chin DJ, Ho YK, Goldstein JL, Brown MS (1983b). Regulation of 3-hydroxy-3-methylglutaryl coenzyme A reductase and its mRNA in rat liver as studied with a monoclonal antibody and a cDNA probe. J Biol Chem 258, 8450–8455.

Liu TF, Tang JJ, Li PS, Shen Y, Li JG, Miao HH, Li BL, Song BL (2012). Ablation of gp78 in liver improves hyperlipidemia and insulin resistance by inhibiting SREBP to decrease lipid biosynthesis. Cell Metab 16, 213–225.

Lloyd-Jones D *et al.* (2009). Heart disease and stroke statistics–2009 update: a report from the American Heart Association Statistics Committee and Stroke Statistics Subcommittee. Circulation 119, 480–486.

Mittelstadt PR, Monteiro JP, Ashwell JD (2012). Thymocyte responsiveness to endogenous glucocorticoids is required for immunological fitness. J Clin Invest 122, 2384–2394.

Nadav E, Shmueli A, Barr H, Gonen H, Ciechanover A, Reiss Y (2003). A novel mammalian endoplasmic reticulum ubiquitin ligase homologous to the yeast Hrd1. Biochem Biophys Res Commun 303, 91–97.

Nakanishi M, Goldstein JL, Brown MS (1988). Multivalent control of 3-hydroxy-3-methylglutaryl coenzyme A reductase. Mevalonate-derived product inhibits translation of mRNA and accelerates degradation of enzyme. J Biol Chem 263, 8929–8937.

Neutzner A, Neutzner M, Benischke AS, Ryu SW, Frank S, Youle RJ, Karbowski M (2011). A systematic search for endoplasmic reticulum (ER) membrane-associated RING finger proteins identifies Nixin/ZNRF4 as a regulator of calnexin stability and ER homeostasis. J Biol Chem 286, 8633–8643.

Palombella VJ, Rando OJ, Goldberg AL, Maniatis T (1994). The ubiquitin-proteasome pathway is required for processing the NF-kappa B1 precursor protein and the activation of NF-kappa B. Cell 78, 773–785.

Pearce MM, Wang Y, Kelley GG, Wojcikiewicz RJ (2007). SPFH2 mediates the endoplasmic reticulum-associated degradation of inositol 1,4,5-trisphosphate receptors and other substrates in mammalian cells. J Biol Chem 282, 20104–20115.

Pearce MM, Wormer DB, Wilkens S, Wojcikiewicz RJ (2009). An endoplasmic reticulum (ER) membrane complex composed of SPFH1 and SPFH2 mediates the ER-associated degradation of inositol 1,4,5-trisphosphate receptors. J Biol Chem 284, 10433–10445.

Persengiev SP, Zhu X, Green MR (2004). Nonspecific, concentration-dependent stimulation and repression of mammalian gene expression by small interfering RNAs (siRNAs). RNA 10, 12–18.

Ravid T, Doolman R, Avner R, Harats D, Roitelman J (2000). The ubiquitin-proteasome pathway mediates the regulated degradation of mammalian 3-hydroxy-3-methylglutaryl-coenzyme A reductase. J Biol Chem 275, 35840–35847.

Roitelman J, Masson D, Avner R, Ammon-Zufferey C, Perez A, Guyon-Gellin Y, Bentzen CL, Niesor EJ (2004). Apomine, a novel hypocholesterolemic agent, accelerates degradation of 3-hydroxy-3-methylglutaryl-coenzyme A reductase and stimulates low density lipoprotein receptor activity. J Biol Chem 279, 6465–6473.

Roitelman J, Olender EH, Bar-Nun S, Dunn WAJ, Simoni RD (1992). Immunological evidence for eight spans in the membrane domain of 3-hydroxy-3-methylglutaryl coenzyme A reductase: implications for enzyme degradation in the endoplasmic reticulum. J Cell Biol 117, 959–973.

Roitelman J, Simoni RD (1992). Distinct sterol and nonsterol signals for the regulated degradation of 3-hydroxy-3-methylglutaryl-CoA reductase. J Biol Chem 267, 25264–25273.

Sanford LP, Kallapur S, Ormsby I, Doetschman T (2001). Influence of genetic background on knockout mouse phenotypes. Methods Mol Biol 158, 217–225.

Semizarov D, Frost L, Sarthy A, Kroeger P, Halbert DN, Fesik SW (2003). Specificity of short interfering RNA determined through gene expression signatures. Proc Natl Acad Sci USA 100, 6347–6352.

Sever N, Song BL, Yabe D, Goldstein JL, Brown MS, DeBose-Boyd RA (2003a). Insig-dependent ubiquitination and degradation of mammalian 3-hydroxy-3-methylglutaryl-CoA reductase stimulated by sterols and geranylgeraniol. J Biol Chem 278, 52479–52490.

Sever N, Yang T, Brown MS, Goldstein JL, DeBose-Boyd RA (2003b). Accelerated degradation of HMG CoA reductase mediated by binding of insig-1 to its sterol-sensing domain. Mol Cell 11, 25–33.

Shmueli A, Tsai YC, Yang M, Braun MA, Weissman AM (2009). Targeting of gp78 for ubiquitin-mediated proteasomal degradation by Hrd1: cross-talk between E3s in the endoplasmic reticulum. Biochem Biophys Res Commun 390, 758–762.

Song BL, Sever N, DeBose-Boyd RA (2005). Gp78, a membrane-anchored ubiquitin ligase, associates with Insig-1 and couples sterol-regulated ubiquitination to degradation of HMG CoA reductase. Mol Cell 19, 829–840.

Steinberg D (2006). Thematic review series: the pathogenesis of atherosclerosis. An interpretive history of the cholesterol controversy, part V: the discovery of the statins and the end of the controversy. J Lipid Res 47, 1339–1351.

Takaishi K, Duplomb L, Wang MY, Li J, Unger RH (2004). Hepatic insig-1 or -2 overexpression reduces lipogenesis in obese Zucker diabetic fatty rats and in fasted/refed normal rats. Proc Natl Acad Sci USA 101, 7106–7111.

Tsai YC *et al*. (2007). The ubiquitin ligase gp78 promotes sarcoma metastasis by targeting KAI1 for degradation. Nat Med 13, 1504–1509.

Tsai YC, Weissman AM (2010). The unfolded protein response, degradation from endoplasmic reticulum and cancer. Genes Cancer 1, 764–778.

Vembar SS, Brodsky JL (2008). One step at a time: endoplasmic reticulum-associated degradation. Nat Rev Mol Cell Biol 9, 944–957.

Wang Y *et al*. (2009). SPFH1 and SPFH2 mediate the ubiquitination and degradation of inositol 1,4,5-trisphosphate receptors in muscarinic receptor-expressing HeLa cells. Biochim Biophys Acta 1793, 1710–1718.

Yamaguchi T, Sharma P, Athanasiou M, Kumar A, Yamada S, Kuehn MR (2005). Mutation of SENP1/SuPr-2 reveals an essential role for desumoylation in mouse development. Mol Cell Biol 25, 5171–5182.

Yang T, Espenshade PJ, Wright ME, Yabe D, Gong Y, Aebersold R, Goldstein JL, Brown MS (2002). Crucial step in cholesterol homeostasis: sterols promote binding of SCAP to INSIG-1, a membrane protein that facilitates retention of SREBPs in ER. Cell 110, 489–500.

ETOC:

HMGCR is subject to Insig-dependent, sterol-accelerated ERAD. gp78 was reported to target HMGCR and Insig-1 for ubiquitination and degradation. Here gp78-mediated Insig-1 degradation is confirmed, but no role for gp78 is found in regulated ERAD of HMGCR. The identity of the HMGCR E3(s) and mechanistic details of HMGCR degradation await further study.